LAWRENCE
LIVERMORE
NATIONAL
LABORATORY

LLNL-SR-454996

Report of visit to LLNL 26 June to 10 July 2010

M. G. Haines

September 14, 2010

Disclaimer

This work performed under the auspices of the U.S. Department of Energy by Lawrence Livermore National Laboratory under Contract DE-AC52-07NA27344.

Report of visit to LLNL
26 June to 10 July 2010

M.G. Haines
Imperial College, London

Summary

On this visit my principal activity was focused on the capsule and in particular to ascertain whether the heat-flow-driven electrothermal (ET) instability would occur in NIF indirect-drive experiments. Filamentary structures, assumed to be associated with the ET instability, have been observed years ago in the coronal plasma of direct-drive[1,2] and more recently by proton probing of targets irradiated directly with an intense short-pulse (~1ps.) laser.[3-6] A different proton probing diagnostic based on a subsidiary exploding pusher source has also shown filamentary structures in direct drive experiments at 10^{13} – 10^{15} W cm^{-2} intensity[7,8], but with only 47μm resolution. Recently measurements have been made on indirectly driven capsules on OMEGA and no filamentary structures were observed[9]. During my visit 1-D numerical simulations from HYDRA were studied. The method was to employ Lagrangian plots of density, temperature etc. for many cells and to test whether the two conditions[10, 11] necessary for growth of the ET instability would simultaneously be satisfied. These conditions are that the electron temperature should be less than a critical temperature and that the electron heat flow should be greater than 0.02 times the free-streaming value. We found that for all of the 16 zones considered none should be unstable, though in some cases it could be marginal. A further development of the heat-flux condition is contained in Appendices A and B, giving a lower threshold, but still indicating that the NIF indirect-drive will be stable to ET.

Other subjects briefly studied included the validity of the non-local model of transport in the hohlraum gas; the inclusion of magnetic fields in HYDRA; the electric field in capsules and shocks; the proposed theta pinch for the LIFE project; the importance of ion viscosity, thermal conduction, and Maxwellisation at the final implosion; the question of an electric field and hence a return current generated in radiation transport due to photon momentum deposition; the physical appropriateness of numerical viscosity; and the magnetic field generation on the gold wall.

1. Introduction to the electrothermal instability

When an electron current exceeds some critical value, an overheating or electrothermal instability can occur. Because short wavelength modes are damped by thermal conduction, and because at long wavelengths the induced electric field caused by the changing magnetic field associated with each filament reduces the current drive, an optimum wavelength for the fastest growth occurs. Indeed no growth occurs if the electron temperature exceeds a critical temperature defined by[10]

$$T_{crit} = \left(\frac{4 n_e e \alpha^c}{3 \mu_0 \kappa^c} \right)^{1/4} \left(\frac{Z \ell n \Lambda_{ei}}{9.7 \times 10^3} \right)^{1/2} \qquad (1)$$

As an example of this temperature, for CH and Z= 3.125, Epperlein and Haines[12] give $\alpha^c = \alpha_0 = 0.3925$ *and* $\kappa^c = \gamma_0 = 6.225$ *and for* $n_e = 10^{29}\, m^{-3}$ *and* $\ell n\Lambda_{ei} = 2$ *gives* $T_{crit} = 145\, eV$.

In the case of the heat-flow driven ET instability, it is the return cold current, driven by the thermoelectric field, which can be unstable[11]. The magnitude of this is proportional to the heat flux q_e, and so the driver for this ET instability can be considered to be the dimensionless nonlinear heat flux, Q, given by

$$Q = \frac{q_e}{n_e m_e v_{Te}^3} = 2.559\left[\frac{m_e(1+b)}{Am_p}\right]^{1/2} \qquad (2)$$

$$\rightarrow 0.0283(1+b)^{1/2} \quad for\ CH\ with\ A = 5.675$$

where $v_{Te}^2 = 2eT_e / m_e$. [Note that this definition of the free-streaming heat flow, $n_e m_e v_{Te}^3$, is $2^{3/2}$ greater than that used by some others.] With ion motion included the ET instability occurs for 0.725 < (1+b) < 3, where b represents the strength of the return current density, insofar, in the model, as it would lead through Joule heating to an electron temperature exceeding 1.32 times the ion temperature. Improved modelling of the ET instability will be discussed later in this report in Appendix A and B.

The main question posed here is whether the ET instability with indirect drive will seed perturbations which exceed the requirements for ignition on NIF.

2. Comparison of 1-D HYDRA simulations with the conditions for the ET instability

The Rev 5 capsule illustrated in fig.1, is $1108\,\mu m$ in radius, the outermost shell of pure CH at 1.069g/cc being $133\,\mu m$ thick. Further layers containing germanium at 0.5%, 1%, 0.5% and 0% were 13, 34, 5 and $5\,\mu m$ in thickness respectively, followed by a $68\,\mu m$ DT ice layer at 0.255g/cc the shell being filled with DT gas at 0.3mg/cc. Assessments of the ET instability were made for zones at 16 depths altogether.

Figs.2 and 3 show plots of R(t) for some of these zones. We start with a Lagrangian zone initially 3.88 μm in depth from the surface, which ablates due to the foot in the laser pulse. Fig.4 shows the radiation temperature T_R(keV), electron temperature T_e(keV) and T_{crit}(keV) as a function of time for the first 10ns. Also shown are the electron number density n_e (10^{23}cm^{-3}), radial velocity v_r(10^7cm/s) and $\ell n\Lambda_{ei}$. The temperature gradient peaks at 1.6ns as shown in fig.5, but while the condition $T_e < T_{crit}$ is satisfied, the dimensionless thermal heat flux Q is 3 x 10^{-5} or only 10^{-2} of that needed to trigger the instability.

The zone at $75.10\,\mu m$ below the surface initially ablates at about 18ns as a result of the main drive. The early three peaks in T_R in fig.6 indicate the earlier shocks, but as in fig.4, the electron temperature rises somewhat later, the main energy flux being radiation transport. The dimensionless heat flux Q is plotted in fig.7 showing a peak at 1.1 x 10^{-4},

well below 1.5×10^{-2} (Eq.(A36) in Appendix A), and only just as T_e increases past T_{crit}. Appendix B gives a lower threshold for Q of 4.6×10^{-3} in Eq.(B11) for CH, but Q is still smaller than this.

At $255.03\,\mu m$ below the ablation surface the zone is in the D-T ice. Fig.8 shows the density rising to a peak at 21.1ns, and T_e is less than T_{crit} up to 21ns. At this time in fig.9 we find that Q is 4×10^{-4} but rises to 6×10^{-3} in a further 0.1ns. Thus this is getting marginal to stability, as Eq.(B10) gives $Q_{crit} = 5.7\times10^{-3}$ for DT.

In conclusion, it is unlikely that the heat flow driven electrothermal instability will occur in the planned indirect-drive capsules on NIF. Experimental confirmation of this favourable result must await 1-50MeV proton probing using protons eminating from the rear surface of a thin foil irradiated by ~ 1ps intense laser pulse. Such measurements will give ~ 12 radiochromic images with $2\,\mu m$ resolution. Meanwhile the protons from exploding pusher capsules at LLE have shown no filamentary structures with $47\,\mu m$ resolution in indirect drive at lower energy[9].

3. Limitations of the present ET model

(i) The present analytic model perturbs an equilibrium in which the Joule heating from the return current balances equipartition to relatively cold ions. The parameter b represents the strength of this term. The model has been extended by Jason Myatt and myself[13] by making the hot electrons *relativistic*, and including a previously omitted electron inertial term. The *competition* between the relativistic resistive Weibel instability and the ET instability was explored in the context of fast ignition. But this is not relevant to the subject of indirect drive.

(ii) A two dimensional computation model using the hybrid *code LSP* gave preliminary results demonstrating the heat-flow driven ET instability[13]. This is currently being extended further by Jason Myatt and myself at LLE. We have been in touch with David Strozzi with the intention of making a joint programme. Furthermore, I have heard recently that radiation transport is now included in LSP, and this code may be relevant to indirect drive as well as to direct drive, fast ignition, and shock ignition.

(iii) The above methodology may underestimate the importance of *faster electrons* preceding the thermal conduction. Non-local transport in 1-D attempts to include this effect, but the simulation from HYDRA used in the present study did not employ this. (There probably was a flux limiter, which is for different physics).

(iv) An *alternative criterion* on the critical heat flux for triggering the ET instability can be derived by noting that the dominant terms in the electron energy equation which were employed in the unperturbed state were J_c^2/σ and the equipartition term $3n_e^2e^3(T_e - T_i)/(m_i\sigma)$. (We note the commonality of the conductivity). The electron heat flux q_e is given by a net enthalpy flow

$$q_e = \frac{5}{2} j_c \left(T_H - T_c \right) \tag{3}$$

where the cold return current density J_c is at a temperature T_c. The hot electron temperature T_H is $3.839T_c$ for linear transport transport in a Lorentz plasma. [In Appendix A the factor of 5/4 is reduced to 1.02]. In nonlocal transport T_H may be considerably higher and reflects the hot temperature ~100 mean free paths away. In addition there are ~30keV electrons arising from SRS in the ionized gas in the hohlraum. All of these require a return cold current to satisfy quasi-neutrality which could be unstable. Eq.(2) was derived from the equilibrium energy balance of Joule heating balancing equipartition. However in the heat flow driven ET instability, the energy source in reality is $-\nabla . \underline{q}$. By distinguishing between the reversible entropy flux and the irreversible heating due to thermal conduction a sounder model using thermodynamic arguments is developed in Appendix B. This gives an even lower value of the critical heat flux that can trigger the ET instability.

4. Photon momentum deposition

In radiation transport, as in the more extreme case of fast ignition, electrons are pushed forward through photon momentum deposition. As a result, an electric field analogous to the thermoelectric field could be set up, given by

$$E_z = \frac{\alpha I}{n_e e c L} \tag{4}$$

(which is eq.(17) in my October 2009 report). Here α is the fraction of the radiation of intensity I absorbed over a length L. This assumes that free electrons are dominant in the absorption rather than atoms. The latter can absorb the photon momentum with no generation of electric field. However for realistic values, the electric field set up in a plasma at solid density is an order of magnitude smaller than that due to ∇T_e. This is in contrast to laser propagation and absorption in the hohlraum gas.

5. Non-local transport in hohlraum gas

Discussions with Rich London and the HYDRA team showed that in general the Schurtz[14] model of non-local transport in 2-D or 3-D would lead the electric field to have a curl, and therefore generate a magnetic field. In the hohlraum gas this model should be used with caution. As stated in my previous visit report, a diode model might be more appropriate for this almost collisionless regime.

6. Ohm's law and magnetic fields in HYDRA

Further discussions with Marty Marinak, Gary Kerbel and Joe Koning were held on including magnetic field generation into HYDRA. Preliminary results with the ∇p_e term in Ohm's law were discussed.

7. The employment of a theta pinch in the LIFE project

At a meeting with the team designing a theta pinch for the LIFE project, I discussed several properties of theta pinches as follows:

(i) Without pre-ionisation, plasma breakdown and formation only occurs as the primary magnetic field goes through zero. This can happen after 1,2 of 3 half cycles of the primary coil. The reason for this probably lies in the energy of the free electrons which are accelerated by the induced electric field. The cross-section for ionisation peaks at a relatively low energy. Electron trajectories and their energy were found in terms of Mathieu functions in ref.15.

(ii) At early times Elton et al[16] found that the plasma breaks up axially into many rings. In fact this was explained as a current driven electrothermal instability in a fully ionised gas[10]. Good agreement was found between the wavelength of the mode and the filling pressure. This and the preceding effects can be avoided with careful pre-ionisation and heating schemes.

(iii) All theta pinches are found to rotate. The origin of this rotation has led to many theories based on

(a) end shorting of the radial electric field and subsequent radial currents and $J_r B_z$ r torque on the plasma (Roberts[17])

(b) axial ejection of oppositely rotating plasmoids (Bostick[18])

(c) radial differential rotation caused by finite ion Larmor radius effects (Velikhov[19])

(d) charge separation and $(\underline{D} \times \underline{H})_\varphi$ r oppositely directed angular momentum in the electromagnetic fields. This is only true at very low plasma density such as employed in early mirror machines. See discussion in the review paper by Haines[20]).

(e) Hall rotation caused by radial perturbing magnetic fields from the collector plate or from imposed Ioffe bars[21]. This work was triggered by Kolb's experiments at NRL, which showed increased rotation and instability.

(f) Initial interaction with the wall[20]. During the first ion Larmor period, momentum is exchanged with the wall in a profential direction. Later results from the 15m long theta pinch at Julich, Germany[22], confirmed that the Doppler shift of spectral lines associated with rotation occurs initially and was of a magnitude agreeing with the formula in ref.20. It was therefore not due to end effects which would be delayed by an Alfvén transit time.

(iv) As a result of the rotation and associated centrifugal force, and, for short theta inches the adverse magnetic field curvature at the ends[23,24], the plasma is unstable. However, there is the possibility of stabilisation of this high β plasma by finite ion Larmor radius effects[25,26].

8. Electric fields in capsules and shocks

Discussions continued with Scott Wilks and Peter Amendt on a more complete description of the electric field set up especially in a shock. This work, to be presented at the 2011 APS-DPP meeting, extends the work of Jaffrin and Probstein[27] and Zel'dovich and Raizer[28] which showed that there is an electron temperature rise preceding the shock, and equilibriation of the ion viscous heating in a thin layer occurs following the shock. Now the thermoelectric term is also included. In addition the LSP code with Fokker-Planck collisions is being applied to obtain a more complete model of a shock. This will be extended to the ablation process in capsules, driven by multiple shocks.

9. Importance of ion viscosity at the final implosion

As a result of the final shock, the ion temperature rises significantly so that the ion mean-free-path is a significant fraction of the final hot-spot radius. This could result in a significant departure from a Maxwellian ion distribution, and affect the high energy ion population which is required for fusion reactions. This could be a major topic for research in the future. Related to this is the use of artificial viscosity in hydrodynamic codes.

References

1. B. Grek et al 1978 *Phys.Rev.Lett.***41**, 1811
2. O. Willi and P.T. Rumsby, 1981 *Optics Commun.***37**, 45
3. M. Borghesi et al, 2001 *Plasma Phys.& Control.Fusion* **43**, A267
4. M. Borghesi et al, 2002 *Phys.Plasmas* **9**, 2214
5. M. Borghesi et al, 2003 *Appl.Phys.Lett.* **82**, 1529
6. M. Boghesi et al, 2003 *Rev.Sci.Instr.* **74**, 1688
7. J.R. Rygg et al, 2008 *Science* **319**, 1223
8. C.K. Li et al, 2007 *Phys.Rev.Lett.* **99,** 015001
9. C.K. Li et al, 2010 *Science.* **327**, 1231
10. M.G. Haines 1974, *J.Plasma Phys.* **12**, 1
11. M.G. Haines 1981, *Phys.Rev.Lett.* **47**, 917
12. E.M. Epperlein & M.G. Haines 1986, *Phys.Fluids* **29**, 1029
13. M.G. Haines & J.F. Myatt, 2007 *Anomalous Absorption Conference*
14. G.P. Schutz et al, 2000 *Phys.Plasmas* **7**, 4238
15. M.G. Haines & D.W. Allan 1963, *Proc.Phys.Soc.* **81**, 104
16. R.H. Dixon, D.F. Düchs & R.C. Elton 1973, *Phys.Fluids* **16**, 1762
17. K.V. Roberts & J.B. Taylor 1962, *Phys.Rev.Lett.* **8**, 197
18. W.H. Bostick & D.R. Wells 1963, *Phys.Fluids* **6** 1325
19. E.P. Velikhov, 1963 *Atomnaya Energiya* **14** 573; 1964 *J. Nucl. Energy C* **6**, 203
20. M.G. Haines 1965, *Advances in Phys.* **14**, 167
21. M.G. Haines 1963, *Phys.Letters* **6**, 313
22. M. Witulski, 1975 *"Experimentelle Untersuchungen zur Erklärung des Ursprungs der Plasmarotation in einem Thetapinch",* Jül-1183-PP, Institut für Plasmaphysik, KFA Jülich, Germany
23. E.C. Bowers 1971, *J.Plasma Phys.* **6**, 80
24. F.A. Haas & J.A. Wesson 1967 *Phys.Fluids* **10** 2245
25. E.C. Bowers & M.G. Haines 1968 *Phys.Fluids* **11** 2695
26. E.C. Bowers & M.G. Haines 1971 *Phys.Fluids* **14** 165
27. M.Y. Jaffrin & R.F. Probstein 1964 *Phys.Fluids* **7** 1658
28. Ya.B. Zel'dovich & Yu.P. Raizer 1966 *"Physics of Shock Waves and High Temperature Hydrodynamic Phenomena" Academic Press (New York & London),* p.515

Appendix A

Criterion for the critical heat flow for a Lorentz plasma

Linear transport for a Lorentz plasma (i.e. neglecting electron-electron collisions which are important for low Z) can be found analytically. See e.g. Epperlein and Haines[12] where the perturbed (vector) electron distribution function in dimensionless form, in absence of a magnetic field, is

$$\underline{F}_1 = F_m(-V^4\,\underline{e} - V^6\underline{t}) \tag{A1}$$

where $F_m = 4\pi v_T^{\,3} f_m / n, V = v/v_T, v_T = (2eT/m)^{1/2}$ and f_m is the Maxwellian distribution function,

$$f_m = \frac{n}{\pi^{3/2} v_T^3}\exp\left(-\frac{v^2}{v_T^2}\right) \tag{A2}$$

Here the dimensionless driving thermodynamic forces are

$$\underline{e} = \frac{2e}{m v_T \nu_T}\underline{E} + \frac{v_T}{\nu_T}\frac{\nabla p}{p} - \frac{5}{2}\frac{v_T}{\nu_T}\frac{\nabla T}{T} \tag{A3}$$

and

$$\underline{t} = \frac{v_T}{\nu_T}\frac{\nabla T}{T} \tag{A4}$$

where $\underline{E}$ is the electric field, p the electron pressure, and ν_T is the mean collision frequency, given by

$$\nu_T = \frac{3\pi^{1/2}}{4\tau_{ei}}$$

and with

$$\tau_{ei} = \frac{3}{4}\left(\frac{m_e}{2\pi}\right)^{1/2}\frac{(4\pi\varepsilon_0)^2 T_e^{3/2}}{Z n_e e^{5/2}\ell n\Lambda_{ei}} \tag{A5}$$

in SI units with T_e in eV. The collision frequency in the Boltzman equation is $v_T^3\nu_T/v^3$. We note that $\underline{e}$ contains not only the electric field and electron pressure gradient but also a ∇T_e term.

We consider only the case of heat flow with zero current flow. The dimensionless current density $\underline{J}$ is given by

$$3\underline{J} = \langle V^5\rangle\underline{e} + \langle V^7\rangle\underline{t} \tag{A6}$$

where

$$\underline{J} = \frac{\underline{j}}{n_e e v_T} = -\frac{1}{3}\int_0^\infty F_1 V^3 dV \tag{A7}$$

and

$$\langle V^m\rangle = \frac{4}{\pi^{1/2}}\int_0^\infty V^{m+2}\exp(-V^2)dV \tag{A8}$$

Forcing $\underline{J}$ to be zero gives a relationship between $\underline{e}$ and $\underline{t}$,

$$\underline{e} = -\frac{\langle V^7 \rangle}{\langle V^5 \rangle}\underline{t} = -4\underline{t} \tag{A9}$$

where $\int_0^\infty V^9 \exp\left(-V^2\right)dV$ *is* 12 *and* $\int_0^\infty V^7 \exp(-V^2)dV$ *is* 3. This then correctly gives the thermoelectric coefficient in Ohm's law as (4-5/2) = 3/2 for Z = ∞.

With the condition (A9) the dimensionless heat flux Z, defined by

$$\underline{Q} = \frac{\underline{q}}{nmv_T{}^3} = \frac{5}{4}\underline{J} + \frac{1}{6}\int_0^\infty \underline{F_1} v^5 dV \tag{A10}$$

becomes for $\underline{J} = 0$,

$$\underline{Q} = -\frac{1}{6}\left[< V^7 > \underline{e} + < V^9 > \underline{t}\right] \tag{A11}$$

$$= -\frac{4}{6\pi^{1/2}}\left[60 - 48\right]\underline{t} = -\frac{8}{\pi^{1/2}}\underline{t} \tag{A12}$$

This correctly gives the heat flux coefficient κ^c *as* 13.58_n $(= 128/3\pi)$ in the formula

$$\underline{q} = -\kappa\nabla T = -\kappa^c \frac{neT}{m}\tau_{ei}\nabla T \tag{A13}$$

$$= -nmv_T{}^3 . \frac{8}{\pi^{1/2}} \cdot \frac{v_T}{3\pi} 4\tau_{ei}\frac{\nabla T}{T} \tag{A14}$$

Whilst the net current density is zero we note that with

$$\underline{F_1} = F_m(4V^4 - V^6)\underline{t} \tag{A15}$$

F_1 is zero at V=2 and for 0<V<2 there is a return "cold" current while for 2<V<∞ there is a "hot" current, equal in magnitude and opposite in sign. We postulate that it is the cold return current density j_c and its associated Joule heating that is the drive for the heat-flow driven electrothermal (ET) instability[11]. In dimensionless form $\underline{J_C}$ is defined by

$$\underline{J_C} = \frac{j_c}{nev_T} = -\frac{1}{3}\int_0^2 \underline{F_1} V^3 dV \tag{A16}$$

$$= -\frac{\underline{t}}{3} \cdot \frac{4}{\pi^{1/2}}\int_0^2 (4V^7 - V^9)\exp(-V^2)dV \tag{A17}$$

$$= \frac{4}{3\pi^{1/2}}\underline{t}\{\frac{4!}{2}\left[1-e^{-4}\left(1+4+\frac{4^2}{2!}+\frac{4^3}{3!}+\frac{4^4}{4!}\right)\right] - 4.\frac{3!}{2}\left[1-e^{-4}\left(1+4+\frac{4^2}{2!}+\frac{4^3}{3!}\right)\right]\}$$

$$= -\frac{2}{3}\cdot\frac{4^4}{\pi^{1/2}}e^{-4}\underline{t} = -1.76358275\underline{t} \qquad \text{(A18)}$$

The fraction of electrons which are "cold", i.e. have 0<V<2, is n_c/n given by

$$\frac{n_C}{n} = \int_0^2 F_m V^2 dV = \frac{4}{\pi^{1/2}}\int_0^2 V^2\exp(-V^2)dV \qquad \text{(A19)}$$

Now the error function can be expanded as follows

$$erf\ x = \frac{2}{\pi^{1/2}}\left\{x\exp\left(-x^2\right)+2\int_0^x t^2\exp\left(-t^2\right)dt\ \right\}$$

$$= \frac{2}{\pi^{1/2}}\left\{x\exp\left(-x^2\right)+\frac{2}{3}x^3\exp\left(-x^2\right)+\frac{4}{3}\int_0^x t^4\exp\left(-t^2\right)dt\ \right\}$$

$$= \frac{2}{\pi^{1/2}}\int_0^x \exp\left(-t^2\right)dt \qquad \text{(A20)}$$

Using this the fraction n_c/n in eq.(A19) can be found as follows

$$\frac{n_C}{n} = erf 2 - \frac{4}{\pi^{1/2}e^4}$$

$$= 0.9953222650_{..} - \frac{4}{\pi^{1/2}e^4}$$

$$= 0.953988294_{...} \qquad \text{(A21)}$$

It follows that the fraction of electrons carrying the "hot" current, n_H/n is $1 - n_C/n = 0.046011706_{..}$ i.e. is less than 5%.

The "cold" temperature T_c can be defined from the cold pressure n_cT_c, namely

$$\frac{n_C T_C}{nT} = \frac{2}{3}\int_0^2 F_m V^4 dV = \frac{8}{3\pi^{1/2}}\int_0^2 V^4\exp(-V^2)dV$$

$$= erf 2 - \frac{2}{\pi^{1/2}}\left(2+\frac{16}{3}\right)\exp(-4) \qquad \text{(A22)}$$

$$= 0.843764372...$$

Hence we find

$$\frac{T_C}{T} = 0.88445988..... \qquad \text{(A23)}$$

Similarly we have the "hot" pressure, $n_HT_H = nT\text{-}n_CT_C$ and hence

$$T_H/T = 3.395562599\ldots \qquad \text{(A24)}$$

$T_H/T_C = 3.839136942\ldots$ (A25)

Or the ratio of the mean-free-paths $\frac{\lambda_{nfpH}}{\lambda_{mfRc}} = \left(\frac{T_H}{T_c}\right)^2 = 14.73897246....$ (A26)

demonstrating the validity of a hybrid model.
This gives

$$\frac{T_H - T_C}{T} = 2.511102719...$$ (A27)

If we equate the dimensionless electron heat flux $\underline{Q}$, given by eq.(A12) to some coefficient β multiplied by $J_0(T_H-T_C)/T$, the coefficient is

$$\beta = \frac{8}{\pi^{1/2}} \times \frac{1}{1.7635... \times 2.5111...} = 1.0191890006....$$ (A28)

i.e.

$\underline{Q} = 1.0192\ldots\ \underline{J}_c\ (T_H-T_C)/T$ (A29)

This contrasts with the formula for $\underline{q}$ in eq.(1) of ref.11, namely $2.5\ j_C\ (T_H-T_C)$ or

$$\underline{Q} = \frac{5}{4}\underline{J}_c\left(\frac{T_H - T_c}{T}\right)$$ (A30)

With ion motion included, the critical T_{eo}/T_I for onset of instability
is $(3+\sqrt{57})/8 = 1.318729304\ldots$ rather than 1.5. From the energy equilibrium,

$$j_c^2 = 3\frac{n^2e^3}{m_i}(T_e - T_i)$$ (A31)

we obtain

$$J_C = \frac{j_c}{nev_T} = \left[\frac{m_e}{2m_i}(1+b)\right]^{1/2}$$ (A32)

where b is defined as $(2T_{oo}-3T_I)/T_{eo}$ (ref.10). The ET instability occurs for

$0.72508278... < (1+b) < 3$ (A33)

Thus the critical dimensionless heat flux Q_{crit} is given by

$Q_{crit} = 2.559288283\ldots\ J_{crit}$ (A34)

$=0.035961517\ldots/A^{1/2}$ (A35)

For CH with $\bar{A} = 5.675$ this gives

$Q_{crit} = 0.015095763$ (A36)

i.e. a flux limiter of 1.5% (or in the LLE definition x $2^{2/3}$ at 4.27%)

Appendix B

Criterion based on thermodynamic arguments

In the model of heat-flow driven ET instability the Joule heating in the current driven ET instability is replaced by $-\nabla q$.. However while $J^2/\sigma T$ is the (positive definite) entropy

production rate, the heat flows term has to be split into the (reversible) entropy flux, q/T, and the irreversible part, i.e.

$$\frac{\nabla q}{T} = -\nabla\cdot\left(\frac{q}{T}\right) - \frac{q.\nabla T}{T^2} \tag{B1}$$

If Fourier's law of heat flow applies, i.e.

$$q = -\kappa\nabla T \tag{B2}$$

the entropy production rate is $\kappa(\nabla T/T)^2$ and is positive definite.

With this argument, and knowing from the current-driven ET instability that the dimensionless current density J_C is given in terms of a parameter b such that the system is unstable for

$$0.7251 < 1+b < 3 \tag{B3}$$

where

$$J_C = \frac{j_c}{nev_T} = \left[\frac{m_e}{2m_i}(1+b)\right]^{1/2} \tag{B4}$$

It follows that for the same irreversible heating rate of plasma from heat flow,

$$\frac{j^2}{\sigma} = \frac{\kappa(\nabla T)^2}{T} = \frac{q^2}{\kappa T} \tag{B5}$$

or

$$j = \frac{q}{T}\cdot\frac{1}{\left(\alpha^c\kappa^c\right)^{1/2}} \tag{B6}$$

using the Braginskii notation in ref.12, where α^c and κ^c are dimensionless parameters which are functions of Z only. The dimensionless heat flux, Q, normalised to the free streaming heat flow nmv_T^3 is thus

$$Q = \frac{q}{nmv_T^3} = \frac{(\alpha^c\kappa^c)}{2}J_c \tag{B7}$$

$$= \frac{(\alpha^c\kappa^c)^{1/2}}{2}\left[\frac{m_e}{2m_i}(1+b)\right]^{1/2} \tag{B8}$$

The critical heat flux Q_{crit} above which the ET instability would grow is, using (B3)

$$Q_{crit} = \frac{(\alpha^c\kappa^c)^{1/2}}{2}\left[\frac{m_e}{2m_i}\cdot 0.7251\right] \tag{B9}$$

For 50:50 DT mixture, $m_i = 2.5\ m_p$, Z=1. $\alpha^c = 0.5061$ and $\kappa^c = 3.203$

$$Q_{crit} = 5.658 \times 10^{-3} \tag{B10}$$

(or 1.6% of LLE defined flux limit).

For CH with $m_i = 5.675\ m_p$, and Z=3.125 we have $\alpha^c = 0.3925$ and $\kappa^c = 6.225$

$$Q_{crit} = 4.610 \times 10^{-3} \tag{B11}$$

(corresponding to a 1.304% flux limit in the LLE definition).

These are lower values of Q_{crit} compared to Appendix A, and could lead to ET instabilities in direct drive.

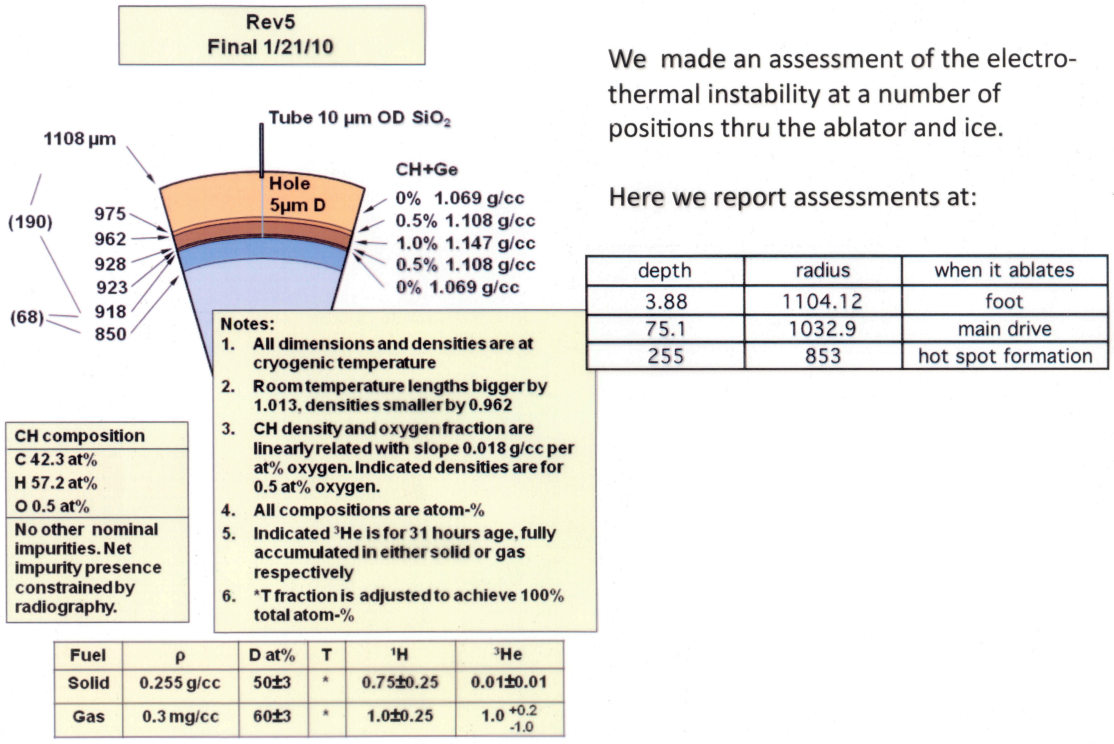

Figure1 The Rev 5 capsule that was examined for the heat-flow driven electrothermal instability.

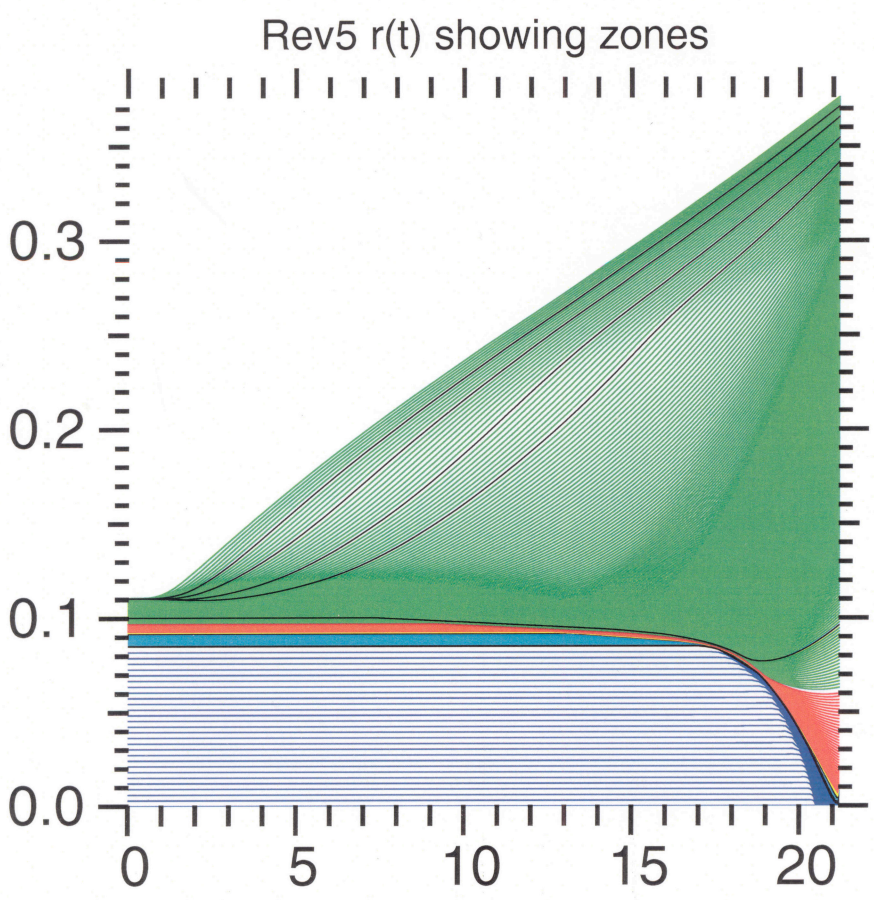

Figure 2 The Lagrangian motion of zones, R(t), for outer zones

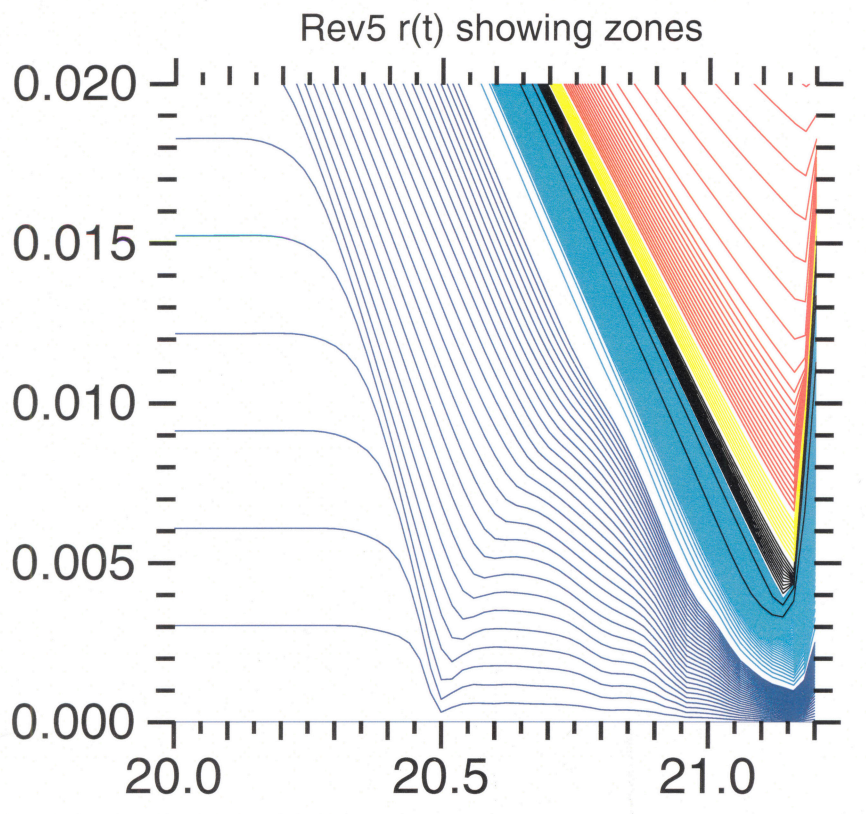

Figure 3. The Lagrangian motion of inner zones, R(t).

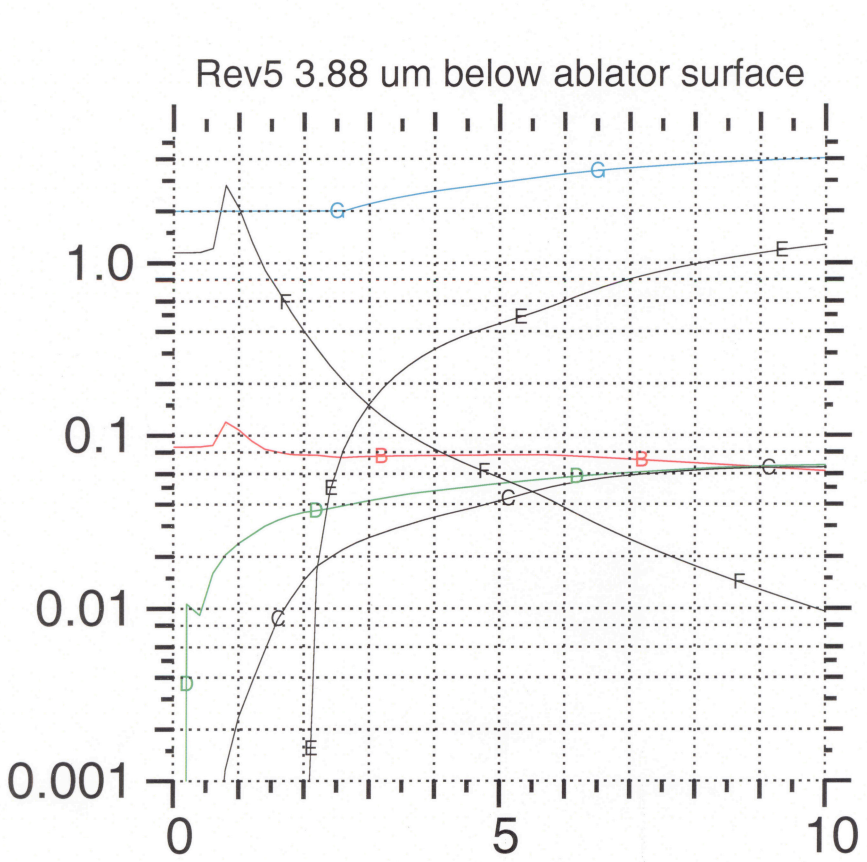

Figure 4. A composite variation with time (ns) of T_R (green D), T_e (black C), T_{crit} (red B), n_e (black F), v_r (black E) and ln Λ_{ei} (blue C), for a zone initially 3.88μm from the surface.

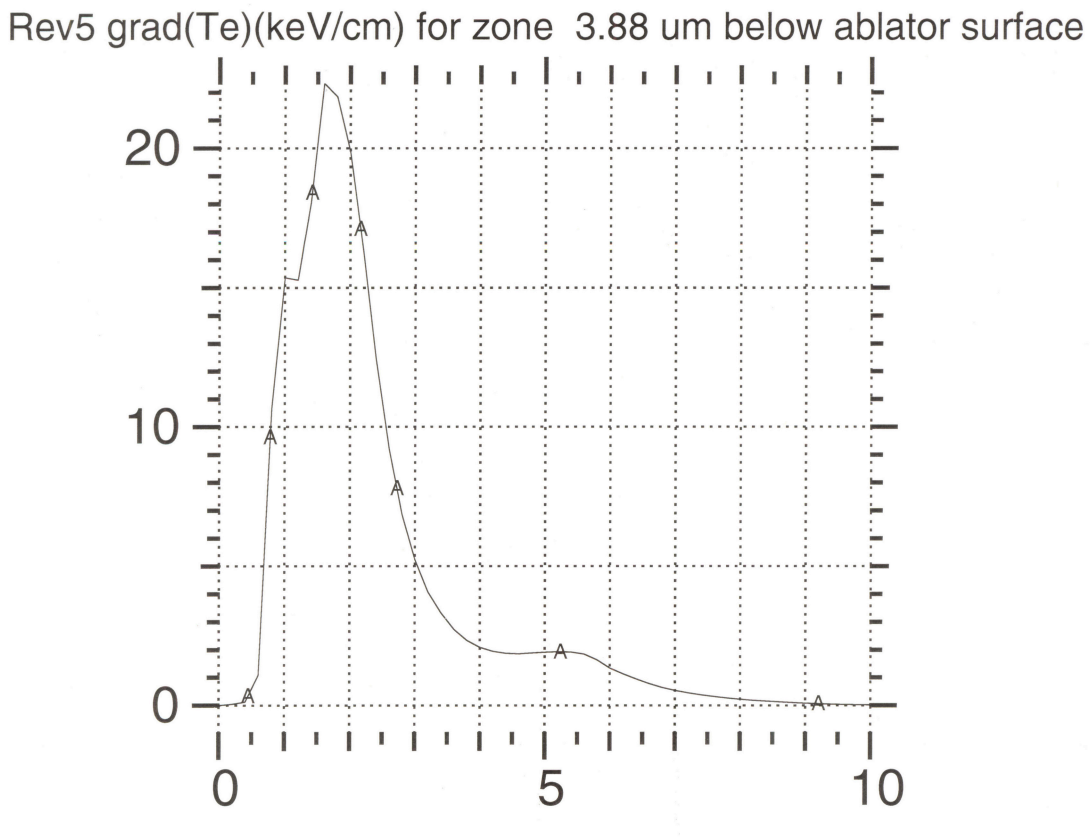

Figure 5. The temperature gradient as a function of time (ns) for the zone initially 3.88μm from the surface.

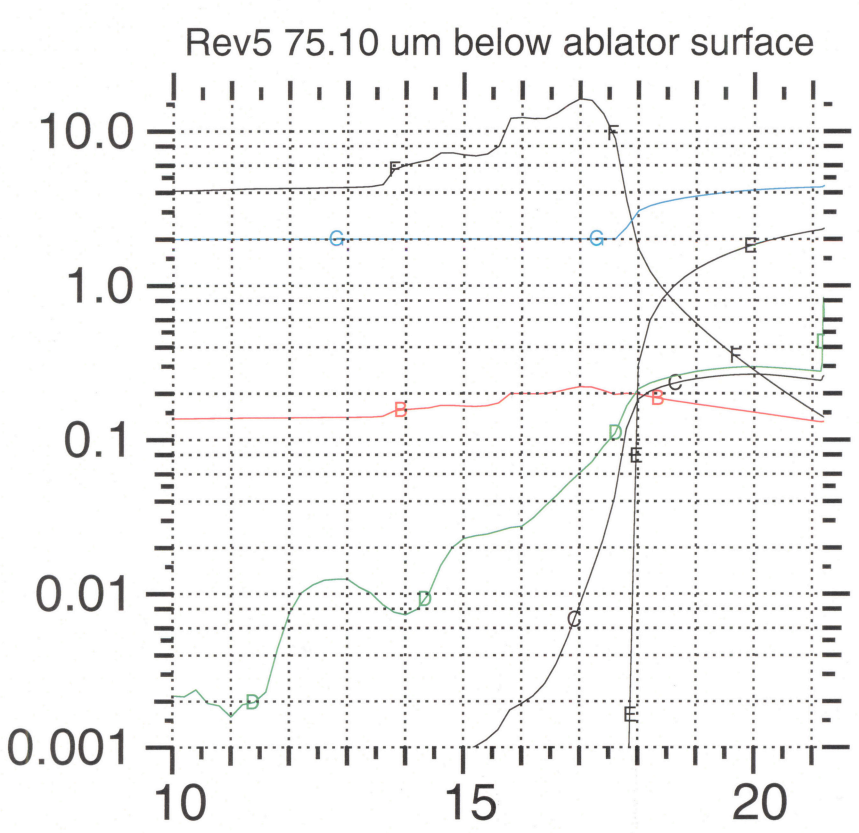

Figure 6. A composite variation with time (ns) of T_R (green D), T_e (black C), T_{crit} (red E), n_e (black F), v_r (black E) and $\ln\Lambda_{ei}$ (blue C), for a zone initially 75.10μm from the surface.

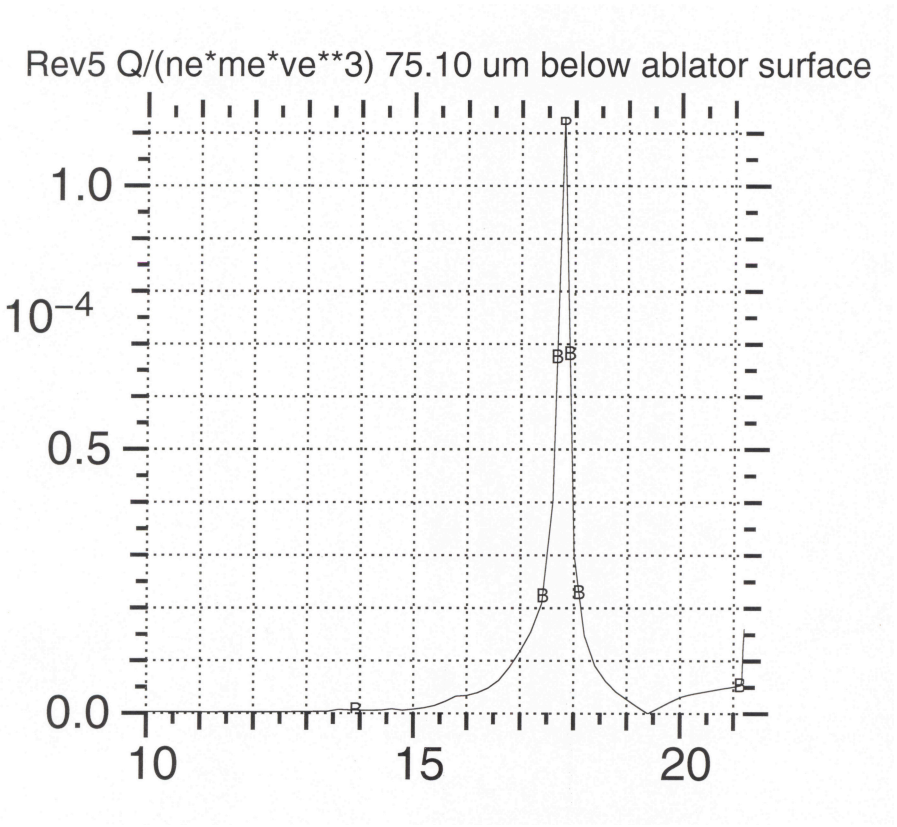

Figure 7. The dimensionless heat-flux Q as a function of time (ns) for the zone initially 75.10μm from the surface.

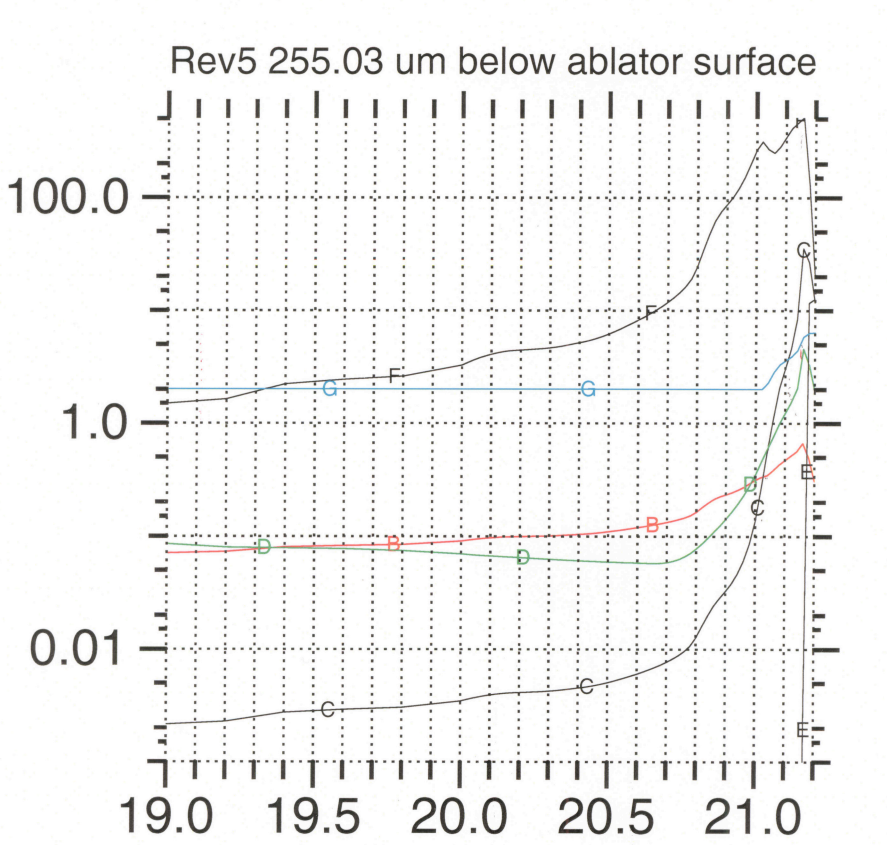

Figure 8. A composite variation in time (ns) of T_R (green D), T_e (black C), T_{crit} (red B), n_e (black F), v_r (black E) and $\ln\Lambda_{ei}$ (blue C) for the zone initially 255.03μm from the surface.

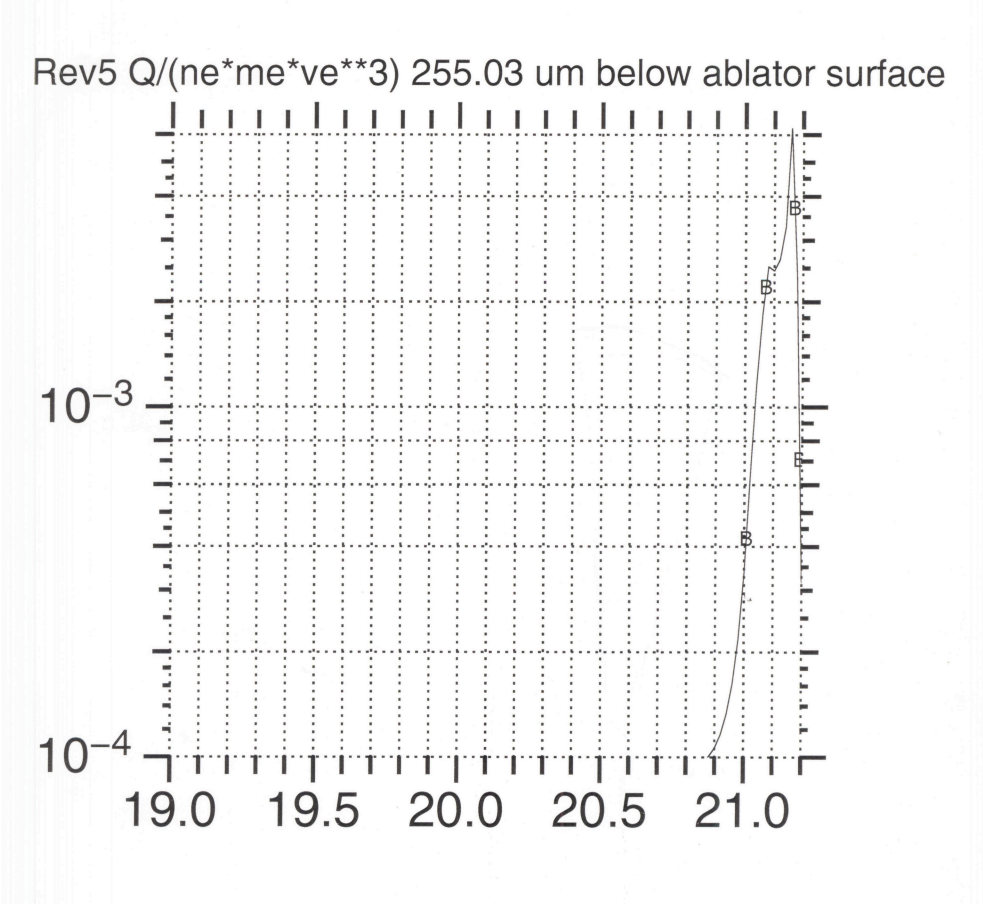

Figure 9. The dimensionless heat-flux Q as a function of time (ns) for the zone initially 255.03μm from the surface.